Supplementary Material

Folic acid and deoxycholic acid derivative modified Fe_3O_4 nanoparticles for efficient pH-dependent drug release and multi-targeted against liver cancer cells

Xiaoyu Wang, [a] Qing Ma, [a] Chaochao Wen, [b] Tao Gong, *[a] Jing Li, [b] Wenting Liang, *[b] Meining Li, [a] Yuyao Wang [a] and Rui Guo*[a]

[a] *Department of Biochemistry and Molecular Biology, Shanxi Medical University, Taiyuan 030001, China; gyt830626@163.com (T. G.); 15834151276@139.com (R. G.)*

[b] *Institute of Environmental Science, Department of Chemistry, Shanxi University, Taiyuan 030006, China; liangwt@sxu.edu.cn (W. L.).*

1. Synthesis of Fe_3O_4 MNPs and APTES-MNPs

Fe_3O_4 MNPs were prepared by chemical deposition method according to our previously reported work [1, 2]. In brief, $FeCl_3 \cdot 6H_2O$ and $FeCl_2 \cdot 4H_2O$ with a molar ratio of 2:1 was dissolved in 500 mL round-bottom flask with secondary water successively, heated to 80 °C under the protection of N_2, and then the pH value of the reaction solution was adjusted with ammonia to about 10, and the reaction was mechanically stirred for half an hour under the condition of 1000 rpm/min. The reaction liquid was cooled to room temperature, separated by hysteresis, the black precipitate was washed with secondary water for three times, and dried overnight in vacuum at 60 °C to obtain Fe_3O_4 MNPs.

150 mg Fe_3O_4 MNPs were added into 300 mL ethanol, and the black particles were all dispersed into ethanol by ultrasonic dispersion. At this time, 60 μL APTES were added under the protection of N_2, and the reaction was mechanically stirred at 1000 rpm/min at room temperature for 12 h. After the reaction, the excess reaction solution was removed, and the supernatant was discarded after hysteresis separation. The black precipitates were washed with anhydrous ethanol for 3 times and vacuum dried at 60 °C to obtain APTES-MNPs.

2. Lagergren's pseudo-first-order kinetic model (Eq (1)) and Ho's pseudo-second-order model (Eq (2))

$$\ln(q_e - q_t) = \ln(q_e) - k_1 t, \quad (1)$$

$$\frac{t}{q_t} = \frac{1}{k_2 q_e^2} + \frac{t}{q_e}, \quad (2)$$

where, in equation (1) and (2): q_e (mg/g) is equilibrium adsorption capacity; q_t (mg/g) is the drug loading at different time points; t (min) is the drug loading time; k_1 and k_2 are kinetic constants.

3. Langmuir model (Eq (3)) and Freundlich model (Eq (4))

$$\frac{C_e}{q_e} = \frac{C_e}{q_m} + \frac{1}{q_m K_L}, \quad (3)$$

$$\ln q_e = \ln K_f + \frac{1}{n} \ln C_e, \quad (4)$$

where, in equation (3) and (4): C_e (mg/L) is the mass concentration at the time of drug loading equilibrium; q_m (mg/g) is the drug load in the saturated state; q_e (mg/g) is the drug load at equilibrium; K_L (L/mg) is the dissociation constant; K_f is the Freundlich constant; 1/n is the Freundlich component factor.

Reference:

[1] T. Gong, Y. H. Zhou, L. L. Sun, W. T. Liang, J. Yang, S. M. Shuang and C. Dong, *RSC Adv.*, 2016, **6**, 80955–80963

[2] T. Gong, R. N. Cheng, X. Y. Wang, et al, *New Journal of Chemistry*, 2021, **45**, 6880-6888.

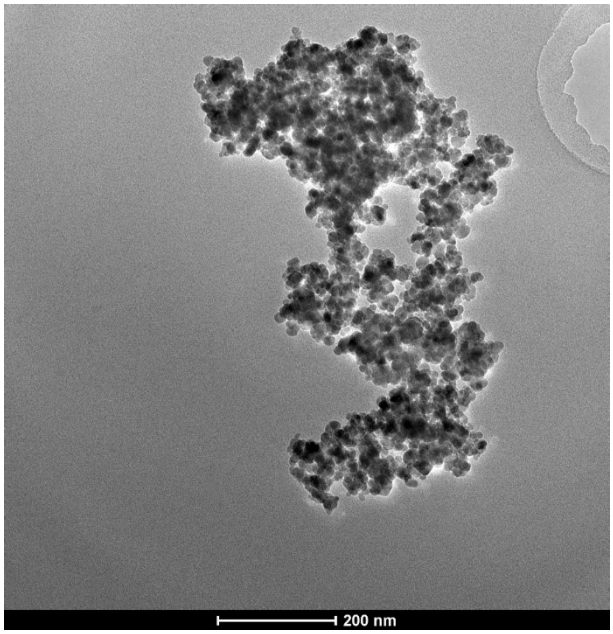

Figure S1. Transmission electron images of Fe_3O_4 MNPs

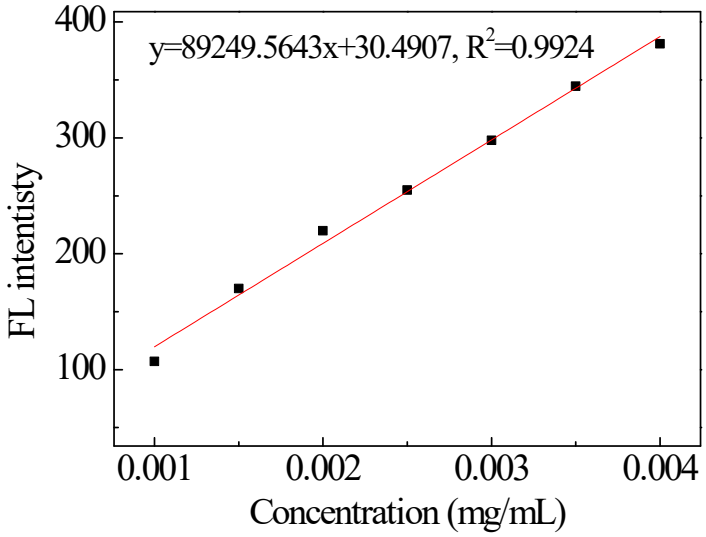

Figure S2. Plot of calibration curves for DOX solution with different concentration.

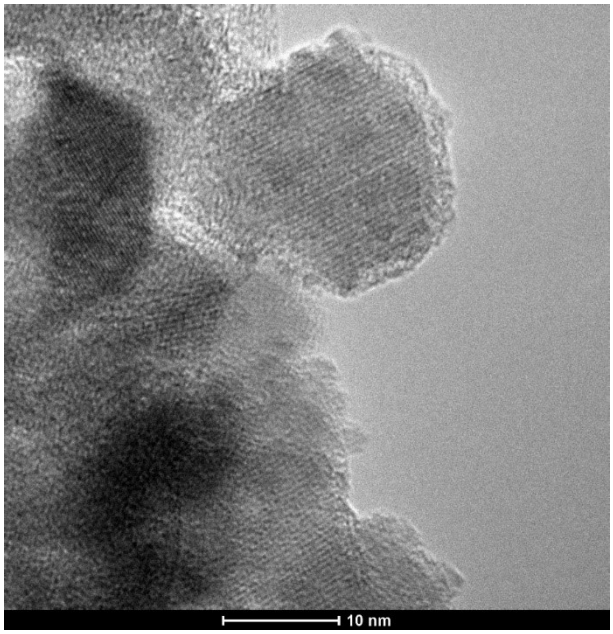

Figure S3. High-resolution transmission electron images of FDCA-FA-MNPs/DOX.

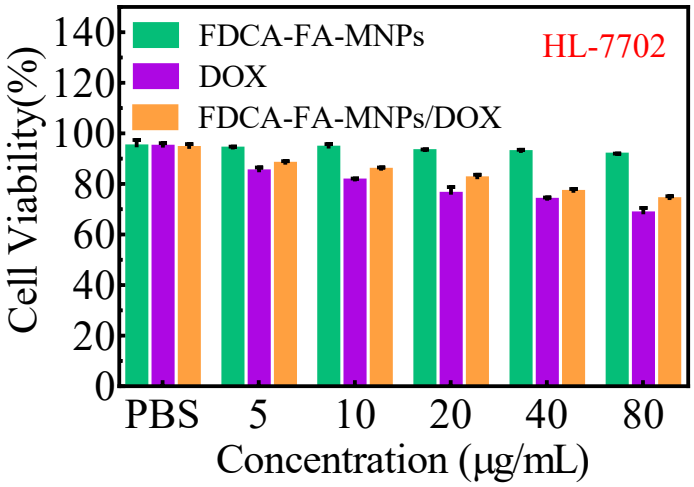

Figure S4. Cell viability of HL-7702 under treated with PBS, FDCA-FA-MNPs, DOX and FDCA-FA-MNPs/DOX. (Among them, the concentrations of FDCA-FA-MNPs and FDCA-FA-MNPs/DOX were 10, 20, 40 and 80 μg mL^{-1}, respectively).

Table S1. The pharmacokinetic parameters of DOX on FDCA-FA-MNPs.

Lagergren's pseudo-first-order kinetic model			Ho's pseudo-second-order kinetic model		
q_e(mg/g)	$k_1(h^{-1})$	R^2	q_e(mg/g)	$k_2(g(mg\cdot h)^{-1})$	R^2
15.23	0.0093	0.8133	79.05	0.0142	0.9994

Table S2. Related parameters of Langmuir isotherm and Freundlich isotherm adsorption models for DOX by FDCA-FA-MNPs.

Langmuir isotherm Model			Freundlich isotherm Model		
q_m(mg/g)	K_L(mg/mL)	R^2	n	K_f(mL/g)	R^2
436.7	0.0439	0.9737	2.625	61.84	0.9994